HHS Public Access

Author manuscript

Neurotoxicology. Author manuscript; available in PMC 2016 September 01.

Published in final edited form as:

Neurotoxicology. 2015 September ; 50: 131–141. doi:10.1016/j.neuro.2015.08.006.

Characterization of binge-dosed methamphetamine-induced neurotoxicity and neuroinflammation

Sarah E.A. McConnell[a], **M. Kerry O'Banion**[a], **Deborah A. Cory-Slechta**[b], **John A. Olschowka**[a], and **Lisa A. Opanashuk**[a,b]

[a] Department of Neurobiology and Anatomy, University of Rochester School of Medicine and Dentistry, 601 Elmwood Ave, Box 603, Rochester, New York 14642, USA

[b] Department of Environmental Medicine, University of Rochester School of Medicine and Dentistry, 601 Elmwood Ave, Box EHSC, Rochester, New York 14642, USA

Abstract

Methamphetamine (MA) is a potent, highly addictive psychostimulant abused by millions of people worldwide. MA induces neurotoxicity, damaging striatal dopaminergic terminals, and neuroinflammation, with striatal glial activation leading to pro-inflammatory cytokine and reactive oxygen species production. It is unclear whether MA-induced neuroinflammation contributes to MA-induced neurotoxicity. In the current study, we examined the linkage between the time course and dose response of MA-induced neurotoxicity and neuroinflammation. Adult male mice underwent a binge dosing regimen of four injections given every two hours with doses of 2, 4, 6, or 8 mg/kg MA per injection, and were sacrificed after 1, 3, 7, or 14 days. Binge MA treatment dose-dependently caused hyperthermia and induced hypoactivity after one day, though activity returned to control levels within one week. Striatal dopamine (DA) was diminished one day after treatment with at least 4 mg/kg MA, while DA turnover rates peaked after seven days. Although striatal tyrosine hydroxylase and DA transporter levels were also decreased one day after treatment with at least 4 mg/kg MA, they trended toward recovery by day 14. All doses of MA activated striatal glia within one day. While astrocyte activation persisted, microglial activation was attenuated over the two weeks of the study. These findings help clarify the relationship between MA-induced neuroinflammation and neurotoxicity, particularly regarding their temporal and dose-specific dynamics.

Keywords

methamphetamine; striatum; neurotoxicity; neuroinflammation; astrocytes; microglia

Corresponding author: Sarah McConnell, SEAMcConnell@gmail.com, 203-213-4908, Present address: 81 Elmerston Road, Rochester, NY 14620.

1. Introduction

Methamphetamine (MA) is a potent and highly addictive psychostimulant, abused by millions of people worldwide (UNODC World Drug Report, 2010). People abuse MA to induce euphoria, and increase energy, attention, and libido. However, long-term MA abuse is associated with a host of systemic and neurological maladies. Systemic afflictions include cardiovascular pathology and liver, kidney, and respiratory failure (Schep et al., 2010). Neurologically, MA abusers exhibit cognitive and psychomotor impairment, and have increased risk for psychosis, strokes, and seizures, with greater drug exposure correlating with greater risk and severity of complications (Simon et al., 2000; Volkow et al., 2001a; Darke et al., 2008).

These impairments are accompanied by neurological damage, particularly in the striatum. Chronic MA abusers have markedly depleted levels of dopamine (DA), tyrosine hydroxylase (TH), and dopamine transporter (DAT) in the striatum (Wilson et al., 1996; Volkow et al., 2001a), indicating damage to dopaminergic axon terminals. Similarly, rodents and non-human primates also exhibit striatal dopaminergic neurotoxicity following MA treatment, characterized by depleted DA, decreased TH and DAT (Wagner et al., 1980; Deng et al., 1999; Harvey et al., 2000), and striatal nerve terminal damage revealed by silver stains (Bowyer et al., 1994; O'Callaghan and Miller, 1994). Interestingly, while the dopaminergic terminals in the striatum are damaged, the cell bodies from which they project in the substantia nigra pars compacta are not destroyed (Harvey et al., 2000): a fact which may account for the capacity for recovery, as well as the rarity of parkinsonian symptoms in MA abusers.

MA induces neurotoxicity via multiple mechanisms, including excitotoxicity, oxidative stress, apoptosis induction, and hyperthermia (Krasnova and Cadet, 2009). Recently, neuroinflammation has been implicated as an additional mechanism. Neuroinflammation has been linked with several neurological disorders, including Alzheimer's disease, Parkinson's disease, multiple sclerosis, and stroke (Czlonkowska and Kurkowska-Jastrzebska, 2011). It is well established that MA exposure activates microglia and astrocytes in culture as well as in animal and human studies (Sheng et al., 1994; Sekine et al., 2008; Krasnova and Cadet, 2009; Yue et al., 2012; Clark et al., 2013). Such gliosis may contribute to MA-induced neurotoxicity, as activated microglia and astrocytes produce reactive oxygen species that are harmful to neurons, and proinflammatory cytokines to propagate the neuroinflammatory cascade and recruit additional immune cells from the periphery, potentially amplifying the oxidative damage to neurons (Clark et al., 2013). However, microglia and astrocytes also serve neuroprotective roles, producing neurotrophic factors, and promoting healing (Czeh et al., 2011; Singh et al., 2011). Furthermore, attempts to prevent MA-induced neurotoxicity by blocking the activation of microglia or astrocytes have yielded contradictory results (Thomas and Kuhn, 2005; Kawasaki et al., 2006; Sriram et al., 2006). Thus, it becomes difficult to define the relationship between the glial activation central to neuroinflammation and the neurotoxicity resulting from MA exposure.

Previous studies have focused on individual doses or time points following MA treatment; however, no comprehensive characterization of the dose-response and time-course of MA-

induced neurotoxicity has yet been published. In this study, we used a binge-dosing paradigm rather than a single injection for MA administration, to more accurately replicate patterns of MA use by human abusers. By administering a wide range of doses (2 to 8 mg/kg MA ×4 injections) and examining several time points (1, 3, 7, and 14 days post-MA), we have characterized the dose-response and time-course of MA-induced striatal dopaminergic terminal damage and glial activation, as well as changes in locomotor behavior, and acute effects on core temperature, to pursue links between MA-induced neuroinflammation and neurotoxicity.

2. Materials and Methods

2.1. Animals

Adult male C57BL/6 mice ordered from Taconic (Germantown, NY), aged 12-14 weeks, were used in this study. Only males were used in order to avoid the confounding effects of different sex hormone profiles between genders and the different phases of the estrous cycle in females, since these differences in sex hormone levels alter susceptibility to methamphetamine-induced neurotoxicity (Yu and Liao, 2000). Mice were maintained on a 12h light:12h dark cycle, with *ad libitum* access to food and water. Data regarding group sample sizes and body mass at sacrifice are shown in Supplementary Table 1. All procedures were approved by the University Committee on Animal Resources of the University of Rochester Medical Center.

2.2. MA Administration and Animal Handling

MA was prepared by the University of Rochester Pharmacy Department. To mimic patterns of MA abuse in humans, we chose to use a binge dosing paradigm, in which mice received a total of four intraperitoneal (i.p.) injections of saline (n = 56) or MA at doses of 2 mg/kg (n = 60), 4 mg/kg (n = 60), 6 mg/kg (n = 72), or 8 mg/kg (n = 72) per injection, administered every two hours. Core body temperatures were recorded prior to the first injection and one hour after each injection using a TH-5 Monitoring Thermometer (Physitemp Instruments, Clifton, NJ). Mice from each treatment group were sacrificed 1 day, 3 days, 7 days, and 14 days following MA treatment via either cervical dislocation for neurotransmitter analysis or transcardial perfusion for immunohistochemical analysis. Following cervical dislocation, the striatum and cortex were dissected, quickly frozen on dry ice, and stored at −80°C. To control for potential inter-hemispheric differences, an equal number of right and left hemispheres from mice in each dose group on each day was used. Transcardial perfusions were performed on mice anesthetized with sodium pentobarbital (Lundbeck Inc., Deerfield, IL), perfusing first with 0.1 M phosphate buffer with 0.25% sodium nitrite and 0.1% sodium heparin (Sigma Aldrich, St. Louis, MS), then with 4% paraformaldehyde in 0.1 M phosphate buffer. Brains were postfixed overnight, then stored in 30% sucrose at 4°C. One mouse from the saline group, one mouse from the 2 mg/kg dose group, two mice from the 4 mg/kg dose group, three mice from the 6 mg/kg dose group, and nine mice from the 8 mg/kg dose group died before their sacrifice dates and therefore were not used for neurotransmitter or immunohistochemical analyses.

2.3. Locomotor Activity

Mice in the 14 day group underwent locomotor activity testing using the Opto-Varimex-Minor (Columbus Instruments, Columbus, OH), which detects horizontal, ambulatory, and vertical movement when a mouse crosses photobeams within the chamber. Horizontal activity was defined as any nonambulatory movement in the X-Y plane, which can include stereotyped movement; ambulatory activity required three successive photobeam breaks in the X-Y plane; and vertical activity was defined as photobeam breaks of the Z plane, such as rearing-related behaviors. Mice were habituated to the testing chamber with three five-minute sessions on each of three consecutive days prior to the start of MA injections. Activity levels from the third day of habituation were used to determine baseline activity for each mouse. The animals' activity levels were assessed one 1, 3 days, 7 days, and 13 days following MA treatment with 45-minute sessions on each testing day.

2.4. High-Performance Liquid Chromatography

Striatal and cortical levels of dopamine and its metabolites metabolites dihydroxyphenylacetic acid (DOPAC) and homovanillic acid (HVA), serotonin (5-HT) and its metabolite 5-hydroxyindoleacetic acid (HIAA), and norepinephrine (NE) were assessed using high-performance liquid chromatography (HPLC; Waters 2695) with electrochemical detection. Tissue samples were placed in perchloric acid (0.1 N), sonicated, and centrifuged at 10,000 × g for 20 minutes before storing supernatants at −80°C. Separation was achieved using the MD-150 Analytical Column (ThermoScientific, 3.2mm × 15cm, 3μm; part no. 70-0636) with commercially available MDTM mobile phase (ThermoScientific; part no. 70-1332) containing 10% acetonitrile, 89% water, and 1% sodium phosphate monobasic monohydrate. Detection occurred with a Water 2465 Electrochemical detector and in-situ silver/silver chloride (ISSAC) electrode maintained at a potential of 0.8 V. Tissue pellets were dissolved in 1 mL of 0.5 N NaOH and total protein content was determined using the Bio-Rad BA protein assay (Hercules, CA). In order to conserve animals and avoid a confounding effect of behavior on neurochemical endpoints, animals used for behavioral testing were omitted from HPLC analysis.

2.5. Immunohistochemistry and Image Analysis

Brains from perfused mice were sectioned at 30 μm on a microtome. The free-floating sections were stored in cryoprotectant (30% sucrose (Sigma Aldrich), 30% ethylene glycol (Sigma Aldrich) in 0.1 M phosphate buffer (PB)) at −20°C until use. Sections were washed with 0.1 M PB and 0.1 M PB with 0.3% Triton X (EMD Biosciences, Inc., San Diego, CA) (PB-Tx). Endogenous peroxidase activity was blocked with 3% hydrogen peroxide, and non-specific binding was blocked with 10% normal goat serum (Millipore, Temecula, CA). Sections were incubated at 4°C overnight with primary antibody: rabbit anti-TH (Millipore, 1:4000), rat anti-DAT (Millipore, 1:1000), rabbit anti-GFAP (Millipore, 1:1000), or rabbit anti-Iba-1 (Wako, Richmond, VA, 1:5000). Following 0.1 M PB washes, sections were incubated in biotinylated goat anti-rabbit or anti-rat secondary antibody (Vector, Burlingame, CA). A Vectastain Elite ABC kit (Vector) was used according to the manufacturer's instructions. The staining was visualized with Sigma Fast 3,3-diaminobenzidine tablets (Sigma-Aldrich). Sections were mounted, dried, coverslipped, and

sealed. Slides were scanned for densitometry using an Epson Perfection 2450 Photo scanner (Long Beach, CA).

Striatal TH and DAT staining density were quantified using ImageJ (NIH, Bethesda, MD) with the experimenter blinded to the treatment conditions. Cortical staining density was used as a background measurement to account for variability during immunohistochemical staining. Values were normalized to their respective saline average to calculate fold change. Striatal astrocyte and microglial activation were quantified using ImageJ to measure the area occupied by GFAP and Iba-1 staining, respectively, with the experimenter blinded to the treatment conditions. Representative photomicrographs were obtained from the central striatum at Bregma 0.3 mm ± 0.2 mm using a Nikon Eclipse 80i microscope (Nikon Instruments, Melville, NY) equipped with a SPOT RT-SE Camera (Model 9.4 Slider-6, Diagnostic Instruments, Sterling Heights, MI) using SPOT Advanced software, version 4.0.9 (Diagnostic Instruments).

2.6. Data Analysis

Locomotor behavior and core temperature data were analyzed with a two-way analysis of variance (ANOVA) with a repeated measure (day of behavioral testing or time of temperature measurement) and an independent factor (MA dose group). Behavioral data from animals that had at least one suspect locomotor reading due to malfunction of the Opto-Varimex-Minor or that died before the end of the experiment were omitted from analysis. HPLC, densitometry, and area occupied data were analyzed with a two-way ANOVA (time × MA dose) without repeated measures. A significant F value was followed with 2-tailed, unpaired Student's t-tests with Bonferroni correction (by multiplying each *p* value by the number of comparisons made) to compare MA-treated groups with the saline control group of the same time point. Results are presented as mean ± SEM. HPLC and densitometry data are graphed as fold change relative to saline baseline, though unnormalized data were used for statistical analysis. Prism 4 was used for statistical analyses. An alpha level of 0.05 was used to determine statistical significance.

3. Results

3.1. MA alters locomotor activity

Mice received i.p. injections of saline or MA at doses of 2, 4, 6, or 8 mg/kg every two hours for four total doses. One day, three days, seven days, and thirteen days later, they underwent locomotor testing to assess horizontal, ambulatory, and vertical motion. A two-way repeated measures ANOVA of horizontal motion revealed a significant effect of MA ($F(4, 140) = 4.95$, $p = 0.0029$), a significant effect of time ($F(4, 140) = 69.21$, $p < 0.0001$), and a significant interaction effect ($F(16, 140)=13.93$, $p < 0.0001$). A two-way repeated measures ANOVA of ambulatory motion revealed a significant effect of MA ($F(4, 140) = 4.61$, $p = 0.0043$), a significant effect of time ($F(4, 140) = 63.65$, $p < 0.0001$), and a significant interaction effect ($F(16, 140) = 11.81$, $p < 0.0001$). A two-way repeated measures ANOVA of vertical motion revealed a significant effect of MA ($F(4, 124) = 2.89$, $p = 0.0384$), a significant effect of time ($F(4, 124) = 22.99$, $p < 0.0001$), and a significant interaction effect ($F(16, 124) = 3.09$, $p = 0.0002$).

Horizontal, ambulatory, and vertical activity levels paralleled each other throughout the time course (Fig. 1). One day following MA treatment, mice given 6 or 8 mg/kg MA exhibited hypoactivity (horizontal motion: 6 mg/kg 777 ± 232 beam breaks, $p < 0.0001$; 8 mg/kg 655 ± 208 beam breaks, $p < 0.0001$; ambulatory motion: saline 5209 ± 596 beam breaks; 6 mg/kg 358 ± 119 beam breaks, $p = 0.0006$; 8 mg/kg 297 ± 127 beam breaks, $p = 0.0005$; vertical motion: saline 275 ± 41 beam breaks; 6 mg/kg 11 ± 6 beam breaks, $p = 0.0173$; 8 mg/kg 10 ± 6 beam breaks, $p = 0.0169$). By seven days after treatment, there were no statistically significant pairwise differences between saline-treated mice and mice in any of the MA-treated groups.

3.2. Binge MA dosing induces hyperthermia

Core body temperature measurements were recorded prior to MA injections and one hour after each MA injection to monitor hyperthermia. A two-way repeated measures ANOVA revealed a significant effect of MA ($F(4, 104) = 13.02$, $p < 0.0001$), a significant effect of time ($F(4, 104) = 17.93$, $p < 0.0001$), and a significant interaction effect ($F(16, 104) = 4.16$, $p < 0.0001$). Mice that received 6 mg/kg MA had significantly raised core temperatures following every MA injection compared with saline-treated mice (1^{st} temperature: 38.2 ± 0.2°C, $p = 0.0124$; 2^{nd}: 37.8 ± 0.3°C, $p = 0.0173$; 3^{rd}: 37.8 ± 0.2°C, $p = 0.0004$; 4^{th}: 38.8°C ± 0.2°C, $p = 0.0003$), and mice in the 8 mg/kg group were significantly hyperthermic following all but the first injection (2^{nd} temperature: 37.8 ± 0.2°C, $p = 0.0038$; 3^{rd}: 38.4 ± 0.3°C, $p = 0.0002$; 4^{th}: 39.3 ± 0.5°C, $p = 0.0143$) (Fig. 2). Mice given 4 mg/kg MA achieved a significant increase in core temperature over controls after the third and fourth injections (3^{rd} temperature: 37.6 ± 0.2°C, $p = 0.0084$; 4^{th}: 38.8 ± 0.2°C, $p = 0.0019$), and mice that received 2 mg/kg MA were hyperthermic following the second and third injections (2^{nd} temperature: 37.3 ± 0.2°C, $p = 0.0486$; 3^{rd}: 37.6 ± 0.2°C, $p = 0.0019$).

3.3. Binge MA dosing alters levels of monoamines and their metabolites in the striatum

Striatal monoamine and metabolite levels were measured by HPLC. MA treatment induced rapid, persistent, and dose-dependent decreases in striatal levels of DA and its metabolites DOPAC and HVA (Fig. 3A, B, C). A two-way ANOVA of striatal DA content revealed a significant effect of MA ($F(4, 85) = 62.42$, $p < 0.0001$), a significant effect of time ($F(2, 85) = 20.46$, $p < 0.0001$), and a significant interaction effect ($F(8, 85) = 6.96$, $p < 0.0001$). Mice given 4, 6, or 8 mg/kg MA showed profoundly decreased DA levels beginning at 1 day (4 mg/kg: 27 ± 8% of control levels, $p = 0.0362$; 6 mg/kg: 28 ± 12% of control levels, $p = 0.0433$; 8 mg/kg: 17 ± 7% of control levels, $p = 0.0200$). A two-way ANOVA of striatal DOPAC levels revealed a significant effect of MA ($F(4, 85) = 71.87$, $p < 0.0001$), a significant effect of time ($F(2, 85) = 10.53$, $p < 0.0001$), and a significant interaction effect ($F(8, 85) = 7.72$, $p < 0.0001$). Striatal DOPAC levels in mice given 4, 6, or 8 mg/kg MA decreased to less than 40% of control striatal DOPAC levels at day 1, and did not recover within seven days (Day 1, 4 mg/kg: 38 ± 10% of control levels, $p = 0.0229$; 6 mg/kg: 32 ± 10% of control levels, $p = 0.0113$; 8 mg/kg: 23 ± 7% of control levels, $p = 0.0051$). Mice given 2 mg/kg MA attained a significant decrease in striatal DOPAC three days after treatment (47 ± 8% of control levels, $p = 0.0027$). A two-way ANOVA of striatal HVA levels revealed a significant effect of MA ($F(4, 85) = 28.09$, $p < 0.0001$), a significant effect of time ($F(2, 85) = 11.02$, $p < 0.0001$), and a significant interaction effect ($F(8, 85) = 4.77$, p

< 0.0001). At day 1, only mice that received 8 mg/kg MA had statistically significantly decreased striatal HVA levels (52 ± 8% control levels, $p = 0.0242$). At day 3, mice in all MA treatment groups had significantly decreased striatal HVA levels (2 mg/kg: 57 ± 6% of control levels, $p = 0.0365$; 4 mg/kg: 21 ± 6% of control levels, $p = 0.0006$; 6 mg/kg: 20 ± 2% of control levels, $p = 0.0022$; 8 mg/kg: 14 ± 3% of control levels, $p = 0.0014$). Striatal HVA levels in mice that received 4, 6, or 8 mg/kg MA remained significantly decreased for the rest of the time course (<50% of control levels, $p < 0.014$).

The highest dose of MA induced a delayed increase in striatal DA turnover rates, quantified as the ratio of the metabolites DOPAC and HVA to DA (Fig. 3D). A two-way ANOVA of striatal DA turnover revealed a significant effect of MA ($F(4, 84) = 18.87$, $p < 0.0001$), a significant effect of time ($F(2, 84)$, 21.07, $p < 0.0001$), and a significant interaction effect ($F(8, 84) = 2.63$, $p = 0.0128$). DA turnover rates peaked at day 7 in the 8 mg/kg group (5.45 ± 0.70 fold greater than control rates, $p = 0.0036$).

MA treatment decreased striatal 5-HT levels in the higher dose groups at days 1, 3, and 7 (Fig. 3E). A two-way ANOVA of striatal 5-HT levels revealed a significant effect of MA ($F(4, 85) = 30.05$, $p < 0.0001$), a significant effect of time ($F(2, 85) = 7.66$, $p = 0.0009$), and a significant interaction effect ($F(8, 85) = 2.75$, $p = 0.0094$). 5-HT levels were significantly decreased in the 8 mg/kg dose group at day 1 (56 ± 7%, $p = 0.0412$), and in the three higher dose groups at day 3 (4 mg/kg: 30 ± 6% of control levels, $p = 0.0088$; 6 mg/kg: 22 ± 1% of control levels, $p = 0.0120$; 8 mg/kg: 38 ± 5% of control levels, $p = 0.0195$). These levels remained significantly decreased at day 7 in the 6 and 8 mg/kg groups (6 mg/kg: 39 ± 11% of control levels, $p = 0.0288$; 8 mg/kg: 34 ± 4% of control levels, $p = 0.0365$).

MA treatment did not consistently alter striatal levels of the 5-HT metabolite HIAA or NE (Fig. 3F, G). A two-way ANOVA of striatal HIAA levels revealed a non-significant effect of MA ($F(4, 85) = 2.02$, $p = 0.0991$), a significant effect of time ($F(2, 85) = 24.73$, $p < 0.0001$), and a significant interaction effect ($F(8, 85) = 3.53$, $p = 0.0014$). A two-way ANOVA of striatal NE levels revealed a significant effect of MA ($F(4, 85) = 9.75$, $p < 0.0001$), a significant effect of time ($F(2, 85) = 9.20$, $p = 0.0002$), and a non-significant interaction effect ($F(8, 85) = 0.88$, $p = 0.5391$). However, there were no statistically significant pairwise differences between any MA group and control levels at any time point for either HIAA or NE.

In contrast to these findings in the striatum, binge MA dosing did not consistently alter levels of monoamines and their metabolites in the cortex (Supplementary Fig. 1).

3.4. Binge MA dosing decreases striatal TH and DAT levels

Striatal sections from mice treated with 0, 2, 4, 6, or 8 mg/kg MA and sacrificed after 1, 3, 7, or 14 days were stained for TH and DAT. MA induced an early, persistent, dose-dependent decrease in striatal TH (Fig. 4). A two-way ANOVA of striatal TH staining intensity revealed a significant effect of MA ($F(4, 102) = 63.32$, $p < 0.0001$), a significant effect of time ($F(3, 102) = 2.90$, $p = 0.0387$), and a significant interaction effect ($F(12, 102) = 3.13$, $p = 0.0008$). MA treatment significantly decreased striatal TH beginning at day 1 in mice given 4 mg/kg (43 ± 9% of control levels, $p = 0.0149$), 6 mg/kg (31 ± 4% of control levels, p

= 0.0001), or 8 mg/kg MA (24 ± 6% of control levels, $p < 0.0001$). These decreases remained statistically significant until day 3 in mice given 4 mg/kg MA (52 ± 17% of control levels, $p = 0.0468$) and day 7 in mice given 6 mg/kg (46 ± 7% of control levels, $p = 0.0016$) or 8 mg/kg MA (20 ± 7% of control levels, $p < 0.0001$).

Similarly, MA induced an early, dose-dependent decrease in striatal DAT that persisted for at least 7 days (Fig. 5). A two-way ANOVA of striatal DAT staining intensity revealed a significant effect of MA ($F(4, 102) = 133.35$, $p < 0.0001$), a significant effect of time ($F(3, 102) = 27.87$, $p < 0.0001$), and a significant interaction effect ($F(12, 102) = 6.00$, $p < 0.0001$). As early as one day following MA, striatal DAT levels were decreased in mice given 4 mg/kg (55 ± 4% of control levels, $p = 0.0008$), 6 mg/kg (36 ± 1% of control levels, $p < 0.0001$), or 8 mg/kg MA (34 ± 4% of control levels, $p < 0.0001$). These decreases persisted until day 3 in mice given 4 mg/kg MA (69 ± 6% of control levels, $p = 0.0191$) and until day 7 in mice given 6 mg/kg (35 ± 5% of control levels, $p = 0.0008$) or 8 mg/kg MA (23 ± 5% of control levels, $p = 0.0004$).

3.5. Binge MA dosing activates glia

Striatal sections were stained for GFAP or Iba-1 to reveal astrocyte and microglial activation, respectively. All doses of MA induced a marked activation of astrocytes at all time points observed (Fig. 6). A two-way ANOVA on the percent of area occupied by GFAP immunoreactivity revealed a significant effect of MA ($F(4, 40) = 13.41$, $p < 0.0001$), a non-significant effect of time ($F(3, 40) = 1.88$, $p = 0.1482$), and a non-significant interaction effect ($F(12, 40) = 1.38$, $p = 0.2147$)(Fig. 6A). Although no pairwise comparisons between saline and MA groups reached statistical significance following the Bonferroni correction, the area occupied by GFAP immunoreactivity in MA-treated mice averaged between 4 and 44 fold greater than that in saline-treated mice. This astrocyte activation is also apparent from the increased number of GFAP-positive astrocytes in the striatum, and the activated morphology of these cells, featuring hypertrophy and increased GFAP immunoreactivity (Fig. 6B).

Similarly, all doses of MA induced dramatic microglial activation one day following treatment; though, unlike the astrocyte response, the microglial activation appeared to attenuate over time (Fig. 7). A two-way ANOVA on the percent of area occupied by Iba-1 immunoreactivity revealed a significant effect of MA ($F(4, 40) = 5.06$, $p = 0.0021$), a significant effect of time ($F(3, 40) = 58.26$, $p < 0.0001$), and a significant interaction effect ($F(12, 40) = 2.61$, $p = 0.0115$)(Fig. 7A). One day following MA treatment, mice given 8 mg/kg MA had significantly more Iba-1 immunoreactivity than mice given saline ($p = 0.0028$). No other pairwise comparisons between MA- and saline-treated mice reached statistical significance following the Bonferroni correction, though on day 1, the mean Iba-1 area occupied in all MA dose groups was at least 78% greater than in saline-treated mice. The morphology of the Iba-1-positive cells reflects this pattern of a rapid increase followed by a gradual decrease in microglial activation (Fig. 7B). One day following MA treatment, striata from mice in all treatment groups exhibited activated microglia with hypertrophic cell bodies, thick processes, and intense Iba-1 immunoreactivity. By day 7, clusters of activated

cells remained scattered throughout the striatum, and microglial activation was not detectable by day 14.

4. Discussion

We have addressed the dose-response and time-course of MA's effects on locomotor behavior, body temperature, striatal dopaminergic terminal markers, and glial activation. We found that binge MA treatment dose-dependently altered locomotor behavior and induced hyperthermia. Indices of striatal neurotoxicity, including decreased DA content, increased DA turnover rates, and depletion of TH and DAT appeared as early as one day following treatment, and persisted throughout the two week time course. Striatal astrocytes and microglia were also activated one day after binge MA treatment in all dose groups. While the astrocyte activation persisted, the microglial response was attenuated over the course of the 14 days. These effects are summarized in Table 1.

Although MA induces acute hyperactivity in mice within the minutes and hours following administration (Itoh et al., 1987; Chen et al., 2012), we observed distinct hypoactivity one day following MA treatment. Grace et al. (2010) reported a comparable effect following a similar MA dosing paradigm, and suggested that this hypoactivity may result from decreased striatal DA content. However, in both Grace's study and the present study, there is a disconnect between locomotor behavior and striatal DA content in that locomotor behavior recovers to control levels while DA levels remain depressed. Perhaps DA depletion accounts for the initial decrease in locomotor activity, and compensatory mechanisms resulting in increased sensitivity to DA allow for behavioral recovery while DA levels remain low. For example, the observed decrease in DAT expression in the striatum may allow prolonged DA signaling by slowing reuptake. It is also possible that one day after binge MA treatment, the animals felt sick from withdrawal symptoms, or were exhausted from their previous hyperactivity, both of which would diminish their locomotor activity.

As expected, binge MA treatment dose-dependently induced hyperthermia in mice. Several other groups have reported that binge MA induces hyperthermia (Bowyer et al., 1994; Grace et al., 2010; Chen et al., 2012), and some suggest that this hyperthermia contributes to MA-induced neurotoxicity. For example, the extent of striatal DA depletion correlates with peak body temperature (Bowyer et al., 1994; Levi et al., 2012); and administering MA at lowered ambient temperatures blocks hyperthermia and attenuates neurotoxicity and microgliosis (Miller and O'Callaghan, 1994; LaVoie and Hastings, 1999; LaVoie et al., 2004). In the present study, we also observed that mice given higher doses of MA had more pronounced hyperthermia and neurotoxicity compared with mice given a lower dose, which is consistent with previous findings.

We observed a marked decrease in striatal DA, DOPAC, and HVA levels, most prominently in the higher dose groups, beginning as early as one day following binge MA treatment, and persisting for at least seven days. These results are consistent with previous observations of MA-induced striatal depletions of DA and its metabolites in mice (Wagner et al., 1980; De Vito and Wagner, 1989; O'Callaghan and Miller, 1994; Sriram et al., 2006). Such DA depletions may contribute to symptoms of MA withdrawal, such as anhedonia and cravings,

serving as negative reinforcement for drug use and leading to relapse (Di Chiara, 1995; Robinson and Berridge, 2008). In the present study, there was also an increase in DA turnover rates, quantified as (DOPAC+HVA)/DA, which peaked at day 7 in the highest dose group. Since DA metabolism by monoamine oxidase is associated with production of hydrogen peroxide (Maker et al., 1981), the increased DA turnover rate may reflect increased oxidative stress in the striatum, secondary to MA's direct effects. Striatal 5-HT was also decreased by the higher doses of MA through at least one week following binge dosing, though these decreases were less severe and required higher doses of MA to reach statistical significance, compared with the MA-induced DA depletion. This discrepancy may reflect differential susceptibility of dopaminergic and serotonergic terminals to MA-induced damage. Dopaminergic terminals are particularly vulnerable, due to DA's ability to auto-oxidize when released from the reducing interior of synaptic vesicles into the cytoplasm, triggering a cascade of oxidative damage (LaVoie and Hastings, 1999; Kuhn et al., 2006; Miyazaki and Asanuma, 2009). In contrast to the striatal neurochemical results, measures of cortical monoamine and metabolite levels showed no apparent trends over the time-course following binge MA treatment. Given monoamine content of the cortex (Goldman-Rakic and Brown, 1982), and the connectivity of the cortex and striatum within the basal ganglia circuitry, we had suspected that the striatal neurochemical response to MA might be reflected in the cortex. However, the MA-induced depletions of 5-HT, DA, and its metabolites, and the increase in DA turnover rate appear to be striatum-specific effects.

We observed marked, dose-dependent decreases in striatal TH and DAT immunohistochemical staining following binge MA dosing. These decreases remained statistically significant up to seven days following treatment. Numerous other studies have also found decreased TH and DAT in the striatum of mice, monkeys, and humans following MA treatment (Wilson et al., 1996; Deng et al., 1999; Harvey et al., 2000). The regional distribution of TH and DAT decreases we observed also matches those reported previously, with greater losses in the dorso-lateral striatum, comparatively little effect in the medial striatum, and no significant effects on the nucleus accumbens (Harvey et al., 2000). Although some groups have questioned whether these decreases reflect nerve terminal damage or simply down-regulation of TH and DAT (Wilson et al., 1996; Harvey et al., 2000), other groups have confirmed MA-induced striatal terminal degeneration via silver staining, using doses of 5 or 10 mg/kg given four times every two hours to rats or mice, respectively (Bowyer et al., 1994; O'Callaghan and Miller, 1994). The apparent recovery of striatal TH and DAT that we observed after two weeks, particularly in mice given 4 or 6 mg/kg, may be due to compensatory upregulation, or nerve terminal regeneration. Additional studies using stains for terminal degeneration would be required to establish whether these changes reflect terminal damage or neuro-regulatory effects.

We observed an effect of MA treatment on markers of striatal astrocyte and microglial activation. While astrocyte activation persisted throughout the course of the study, microglial activation subsided with time, leaving scattered clusters of activated cells at day seven, and returning to control levels by day 14. These temporal kinetics are similar to what other groups using binge dosing paradigms have reported (O'Callaghan and Miller, 1994; LaVoie et al., 2004; Thomas et al., 2004b). Although MA-induced glial activation is a well-

established phenomenon *in vitro*, in rodents, and in humans (Sheng et al., 1994; Lau et al., 2000; Thomas et al., 2004a; Sekine et al., 2008; Yue et al., 2012; Clark et al., 2013), its role in MA-induced neurotoxicity is uncertain. Microglial activation precedes MA-induced dopaminergic terminal damage by one day in rats, suggesting that microglial activation could contribute to neural damage, rather than responding to it (LaVoie et al., 2004); and inhibiting microglial activation with MK-801 or dextromethorphan attenuates MA-induced DA depletion, though these agents also prevent hyperthermia, which may account for their neuroprotective effect (Thomas and Kuhn, 2005). Several studies have shown that treatment with anti-inflammatory agents attenuates MA-induced gliosis and neurotoxicity in the striatum (Asanuma et al., 2004; Zhang et al., 2006; Hashimoto et al., 2007) and hippocampus (Goncalves et al., 2010). Conversely, amplifying local neuroinflammation via intrastriatal administration of lipopolysaccharide exacerbated MA-induced dopaminergic neurotoxicity (Jung et al., 2010). However, Sriram et al. (2006) found that minocycline treatment prevented microglial activation, but did not alter astrocyte activation and failed to protect against MA-induced striatal dopaminergic damage. Similarly, Kawasaki et al. (2006) found that MA-induced dopaminergic neurotoxicity could be blocked using the radical scavenger edaravone despite unaltered microglial activation. We carried out correlational analysis on our data for measures of glial activation and neurotoxicity, but we did not find statistically significant correlation across doses. This may be due to the incongruity between the relatively flat dose-response curve of the glial activation response and more linear curve of the neurotoxicity effect. In the current study, mice in the lowest dose group appeared to exhibit glial activation one day after treatment, as did mice in the higher dose groups; however, mice in the lowest dose group did not exhibit significant decreases in striatal DA, TH, or DAT. One possible reason for this apparent discrepancy is that low-dose MA elicits sufficient damage of terminals to locally activate glia, but not result in measurable loss of TH or DAT staining.

In the current study, we found that binge MA treatment in mice dose-dependently alters locomotor behavior, causes hyperthermia, and induces striatum-specific dopaminergic neurotoxicity accompanied by neuroinflammation, with dopaminergic terminal marker depletion and astrocyte activation persisting for at least two weeks following treatment. The complex interactions and contributions, whether neurotoxic or neuroprotective, of astrocytes and microglia following MA exposure remain ambiguous. As we deepen our understanding of these processes, we can pursue mechanisms of recovery and develop therapeutic options for people suffering from MA-induced neurotoxicity.

Supplementary Material

Refer to Web version on PubMed Central for supplementary material.

Acknowledgements

We are grateful to Bryan Thompson, Diana Navarro, and Jack Walter for their assistance with animal handling. We also thank Douglas Weston and Sue Liu for their help with behavioral testing and HPLC, respectively. This work was supported by a grant from the National Institutes of Health (R01 DA026009).

References

Asanuma M, Miyazaki I, Higashi Y, Tsuji T, Ogawa N. Specific gene expression and possible involvement of inflammation in methamphetamine-induced neurotoxicity. Ann N Y Acad Sci. 2004; 1025:69–75. [PubMed: 15542702]

Bowyer JF, Davies DL, Schmued L, Broening HW, Newport GD, Slikker W Jr. Holson RR. Further studies of the role of hyperthermia in methamphetamine neurotoxicity. J Pharmacol Exp Ther. 1994; 268:1571–1580. [PubMed: 8138969]

Chen H, Wu J, Zhang J, Fujita Y, Ishima T, Iyo M, Hashimoto K. Protective effects of the antioxidant sulforaphane on behavioral changes and neurotoxicity in mice after the administration of methamphetamine. Psychopharmacology (Berl.). 2012; 222:37–45. [PubMed: 22200890]

Clark KH, Wiley CA, Bradberry CW. Psychostimulant Abuse and Neuroinflammation: Emerging Evidence of Their Interconnection. Neurotox Res. 2013; 23:174–188. [PubMed: 22714667]

Czeh M, Gressens P, Kaindl AM. The yin and yang of microglia. Dev Neurosci. 2011; 33:199–209. [PubMed: 21757877]

Czlonkowska A, Kurkowska-Jastrzebska I. Inflammation and gliosis in neurological diseases--clinical implications. J Neuroimmunol. 2011; 231:78–85. [PubMed: 20943275]

Darke S, Kaye S, McKetin R, Duflou J. Major physical and psychological harms of methamphetamine use. Drug Alcohol Rev. 2008; 27:253–262. [PubMed: 18368606]

De Vito MJ, Wagner GC. Methamphetamine-induced neuronal damage: a possible role for free radicals. Neuropharmacology. 1989; 28:1145–1150. [PubMed: 2554183]

Deng X, Ladenheim B, Tsao LI, Cadet JL. Null mutation of c-fos causes exacerbation of methamphetamine-induced neurotoxicity. J Neurosci. 1999; 19:10107–10115. [PubMed: 10559418]

Di Chiara G. The role of dopamine in drug abuse viewed from the perspective of its role in motivation. Drug Alcohol Depend. 1995; 38:95–137. [PubMed: 7671769]

Flora G, Lee YW, Nath A, Maragos W, Hennig B, Toborek M. Methamphetamine-induced TNF-alpha gene expression and activation of AP-1 in discrete regions of mouse brain: potential role of reactive oxygen intermediates and lipid peroxidation. Neuromolecular Med. 2002; 2:71–85. [PubMed: 12230306]

Goldman-Rakic PS, Brown RM. Postnatal development of monoamine content and synthesis in the cerebral cortex of rhesus monkeys. Brain Res. 1982; 256:339–349. [PubMed: 7104766]

Goncalves J, Martins T, Ferreira R, Milhazes N, Borges F, Ribeiro CF, Malva JO, Macedo TR, Silva AP. Methamphetamine-induced early increase of IL-6 and TNF-alpha mRNA expression in the mouse brain. Ann N Y Acad Sci. 2008; 1139:103–111. [PubMed: 18991854]

Goncalves J, Baptista S, Martins T, Milhazes N, Borges F, Ribeiro CF, Malva JO, Silva AP. Methamphetamine-induced neuroinflammation and neuronal dysfunction in the mice hippocampus: preventive effect of indomethacin. Eur J Neurosci. 2010; 31:315–326. [PubMed: 20074221]

Grace CE, Schaefer TL, Herring NR, Graham DL, Skelton MR, Gudelsky GA, Williams MT, Vorhees CV. Effect of a neurotoxic dose regimen of (+)-methamphetamine on behavior, plasma corticosterone, and brain monoamines in adult C57BL/6 mice. Neurotoxicol Teratol. 2010; 32:346–355. [PubMed: 20096350]

Harvey DC, Lacan G, Tanious SP, Melega WP. Recovery from methamphetamine induced long-term nigrostriatal dopaminergic deficits without substantia nigra cell loss. Brain Res. 2000; 871:259–270. [PubMed: 10899292]

Hashimoto K, Tsukada H, Nishiyama S, Fukumoto D, Kakiuchi T, Iyo M. Protective effects of minocycline on the reduction of dopamine transporters in the striatum after administration of methamphetamine: a positron emission tomography study in conscious monkeys. Biological Psychiatry. 2007; 61:577–581. [PubMed: 16712806]

Itoh T, Murai S, Yoshida H, Masuda Y, Saito H, Chen CH. Effects of methamphetamine and morphine on the vertical and horizontal motor activities in mice. Pharmacol Biochem Behav. 1987; 27:193–197. [PubMed: 3615543]

Jung BD, Shin EJ, Nguyen XK, Jin CH, Bach JH, Park SJ, Nah SY, Wie MB, Bing G, Kim HC. Potentiation of methamphetamine neurotoxicity by intrastriatal lipopolysaccharide administration. Neurochem Int. 2010; 56:229–244. [PubMed: 19850096]

Kawasaki T, Ishihara K, Ago Y, Nakamura S, Itoh S, Baba A, Matsuda T. Protective effect of the radical scavenger edaravone against methamphetamine-induced dopaminergic neurotoxicity in mouse striatum. Eur J Pharmacol. 2006; 542:92–99. [PubMed: 16784740]

Krasnova IN, Cadet JL. Methamphetamine toxicity and messengers of death. Brain Res Rev. 2009; 60:379–407. [PubMed: 19328213]

Kuhn DM, Francescutti-Verbeem DM, Thomas DM. Dopamine quinones activate microglia and induce a neurotoxic gene expression profile: relationship to methamphetamine-induced nerve ending damage. Ann N Y Acad Sci. 2006; 1074:31–41. [PubMed: 17105901]

Lau JW, Senok S, Stadlin A. Methamphetamine-induced oxidative stress in cultured mouse astrocytes. Ann N Y Acad Sci. 2000; 914:146–156. [PubMed: 11085317]

LaVoie MJ, Hastings TG. Dopamine quinone formation and protein modification associated with the striatal neurotoxicity of methamphetamine: evidence against a role for extracellular dopamine. J Neurosci. 1999; 19:1484–1491. [PubMed: 9952424]

LaVoie MJ, Card JP, Hastings TG. Microglial activation precedes dopamine terminal pathology in methamphetamine-induced neurotoxicity. Exp Neurol. 2004; 187:47–57. [PubMed: 15081587]

Levi MS, Divine B, Hanig JP, Doerge DR, Vanlandingham MM, George NI, Twaddle NC, Bowyer JF. A comparison of methylphenidate-, amphetamine-, and methamphetamine-induced hyperthermia and neurotoxicity in male Sprague-Dawley rats during the waking (lights off) cycle. Neurotoxicol Teratol. 2012; 34:253–262. [PubMed: 22289608]

Maker HS, Weiss C, Silides DJ, Cohen G. Coupling of dopamine oxidation (monoamine oxidase activity) to glutathione oxidation via the generation of hydrogen peroxide in rat brain homogenates. J Neurochem. 1981; 36:589–593. [PubMed: 7463078]

Miller DB, O'Callaghan JP. Environment-, drug- and stress-induced alterations in body temperature affect the neurotoxicity of substituted amphetamines in the C57BL/6J mouse. J Pharmacol Exp Ther. 1994; 270:752–760. [PubMed: 8071868]

Miyazaki I, Asanuma M. Approaches to prevent dopamine quinone-induced neurotoxicity. Neurochem Res. 2009; 34:698–706. [PubMed: 18770028]

O'Callaghan JP, Miller DB. Neurotoxicity profiles of substituted amphetamines in the C57BL/6J mouse. J Pharmacol Exp Ther. 1994; 270:741–751. [PubMed: 8071867]

Robinson TE, Berridge KC. The incentive sensitization theory of addiction: some current issues. Phil Trans R Soc B. 2008; 363:3137–3146. [PubMed: 18640920]

Schep LJ, Slaughter RJ, Beasley DM. The clinical toxicology of metamfetamine. Clin Toxicol (Phila.). 2010; 48:675–694. [PubMed: 20849327]

Sekine Y, Ouchi Y, Sugihara G, Takei N, Yoshikawa E, Nakamura K, Iwata Y, Tsuchiya KJ, Suda S, Suzuki K, Kawai M, Takebayashi K, Yamamoto S, Matsuzaki H, Ueki T, Mori N, Gold MS, Cadet JL. Methamphetamine causes microglial activation in the brains of human abusers. J Neurosci. 2008; 28:5756–5761. [PubMed: 18509037]

Sheng P, Cerruti C, Cadet JL. Methamphetamine (METH) causes reactive gliosis in vitro: attenuation by the ADP-ribosylation (ADPR) inhibitor, benzamide. Life Sci. 1994; 55:PL51–54. [PubMed: 8007755]

Simon SL, Domier C, Carnell J, Brethen P, Rawson R, Ling W. Cognitive impairment in individuals currently using methamphetamine. Am J Addict. 2000; 9:222–231. [PubMed: 11000918]

Singh S, Swarnkar S, Goswami P, Nath C. Astrocytes and microglia: responses to neuropathological conditions. Int J Neurosci. 2011; 121:589–597. [PubMed: 21827229]

Sriram K, Miller DB, O'Callaghan JP. Minocycline attenuates microglial activation but fails to mitigate striatal dopaminergic neurotoxicity: role of tumor necrosis factor-alpha. J Neurochem. 2006; 96:706–718. [PubMed: 16405514]

Thomas DM, Dowgiert J, Geddes TJ, Francescutti-Verbeem D, Liu X, Kuhn DM. Microglial activation is a pharmacologically specific marker for the neurotoxic amphetamines. Neurosci Lett. 2004a; 367:349–354. [PubMed: 15337264]

Thomas DM, Walker PD, Benjamins JA, Geddes TJ, Kuhn DM. Methamphetamine neurotoxicity in dopamine nerve endings of the striatum is associated with microglial activation. J Pharmacol Exp Ther. 2004b; 311:1–7. [PubMed: 15163680]

Thomas DM, Kuhn DM. MK-801 and dextromethorphan block microglial activation and protect against methamphetamine-induced neurotoxicity. Brain Res. 2005; 1050:190–198. [PubMed: 15987631]

UNODC, World Drug Report. United Nations Publication; 2010. Sales No. E.10.XI.13

Volkow ND, Chang L, Wang GJ, Fowler JS, Leonido-Yee M, Franceschi D, Sedler MJ, Gatley SJ, Hitzemann R, Ding YS, Logan J, Wong C, Miller EN. Association of dopamine transporter reduction with psychomotor impairment in methamphetamine abusers. Am J Psychiatry. 2001a; 158:377–382. [PubMed: 11229977]

Volkow ND, Chang L, Wang GJ, Fowler JS, Franceschi D, Sedler M, Gatley SJ, Miller E, Hitzemann R, Ding YS, Logan J. Loss of dopamine transporters in methamphetamine abusers recovers with protracted abstinence. J Neurosci. 2001b; 21:9414–9418. [PubMed: 11717374]

Wagner GC, Ricaurte GA, Seiden LS, Schuster CR, Miller RJ, Westley J. Long-lasting depletions of striatal dopamine and loss of dopamine uptake sites following repeated administration of methamphetamine. Brain Res. 1980; 181:151–160. [PubMed: 7350950]

Wilson JM, Kalasinsky KS, Levey AI, Bergeron C, Reiber G, Anthony RM, Schmunk GA, Shannak K, Haycock JW, Kish SJ. Striatal dopamine nerve terminal markers in human, chronic methamphetamine users. Nat Med. 1996; 2:699–703. [PubMed: 8640565]

Yu, Liao. Sexual differences and estrous cycle in methamphetamine-induced dopamine and serotonin depletions in the striatum of mice. J Neural Transm. 2000; 107:419–427. [PubMed: 11215753]

Yue X, Qiao D, Wang A, Tan X, Li Y, Liu C, Wang H. CD200 attenuates methamphetamine-induced microglial activation and dopamine depletion. J Huazhong Univ Sci Technolog Med Sci. 2012; 32:415–421. [PubMed: 22684568]

Zhang L, Kitaichi K, Fujimoto Y, Nakayama H, Shimizu E, Iyo M, Hashimoto K. Protective effects of minocycline on behavioral changes and neurotoxicity in mice after administration of methamphetamine. Prog Neuropsychopharmacol Biol Psychiatry. 2006; 30:1381–1393. [PubMed: 16839653]

Highlights

- Higher doses of MA rapidly decreased striatal DA.
- Higher doses of MA rapidly and non-persistently decreased striatal TH and DAT.
- A wide range of doses of MA activated striatal glia.
- Astrocyte activation persisted, but microglial activation declined over 14 days.

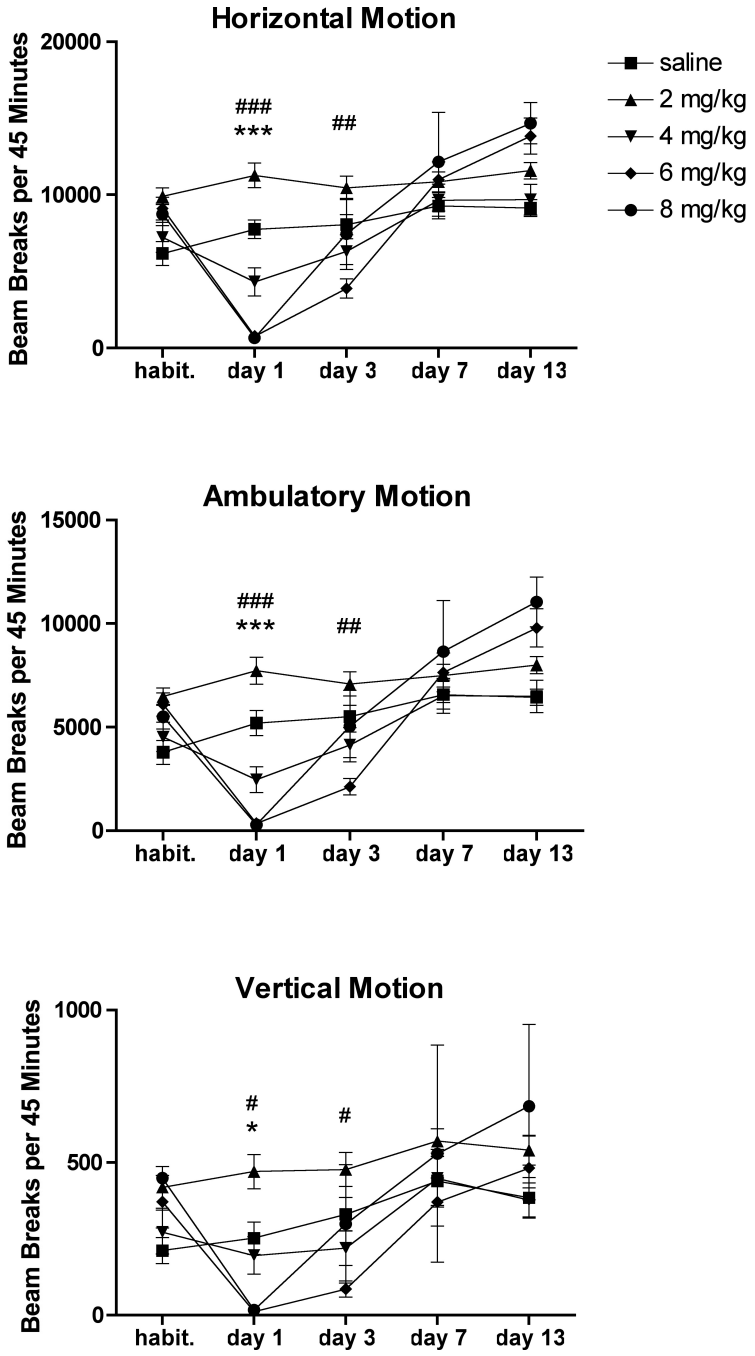

Figure 1.

Binge MA dosing alters locomotor activity. MA dose-dependently decreased horizontal, ambulatory, and vertical motion one day after treatment. This effect was attenuated within 7 days. Data are presented as mean ± SEM (n = 10 per dose group). “Habit.” refers to the third day of habituation. * or *** $p < 0.05$ or 0.001 for 8 mg/kg MA compared with saline group; #, ##, or ### $p < 0.05$, 0.01, or 0.005 for 6 mg/kg compared with saline group.

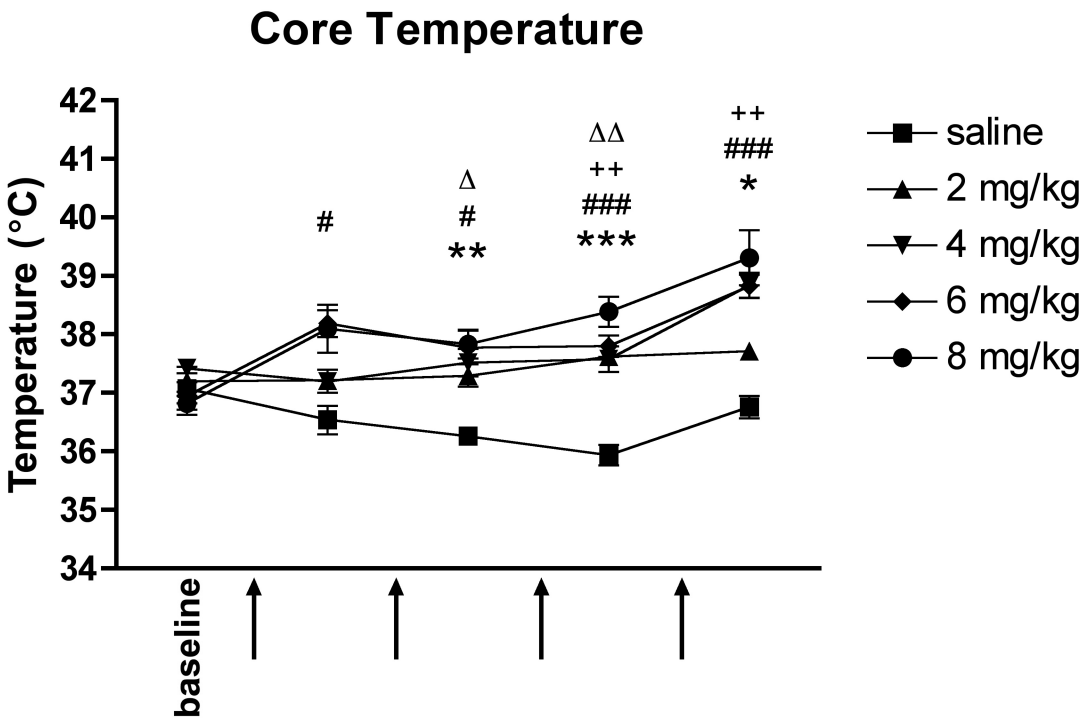

Figure 2.

Binge MA dosing induces hyperthermia. Mice in all dose groups had significantly raised body temperatures during the course of MA injections, though only mice given at least 4 mg/kg MA remained significantly hyperthermic following the final injection. Data are presented as mean ± SEM (n = 5-8 per dose group). Arrows indicate injection times. *, **, or *** $p < 0.05$, 0.01, or 0.001 for 8 mg/kg MA compared with saline; # or ### $p < 0.05$ or 0.001 for 6 mg/kg MA compared with saline; ++ $p < 0.01$ for 4 mg/kg MA compared with saline; Δ or ΔΔ $p < 0.05$ or 0.01 for 2 mg/kg compared with saline group.

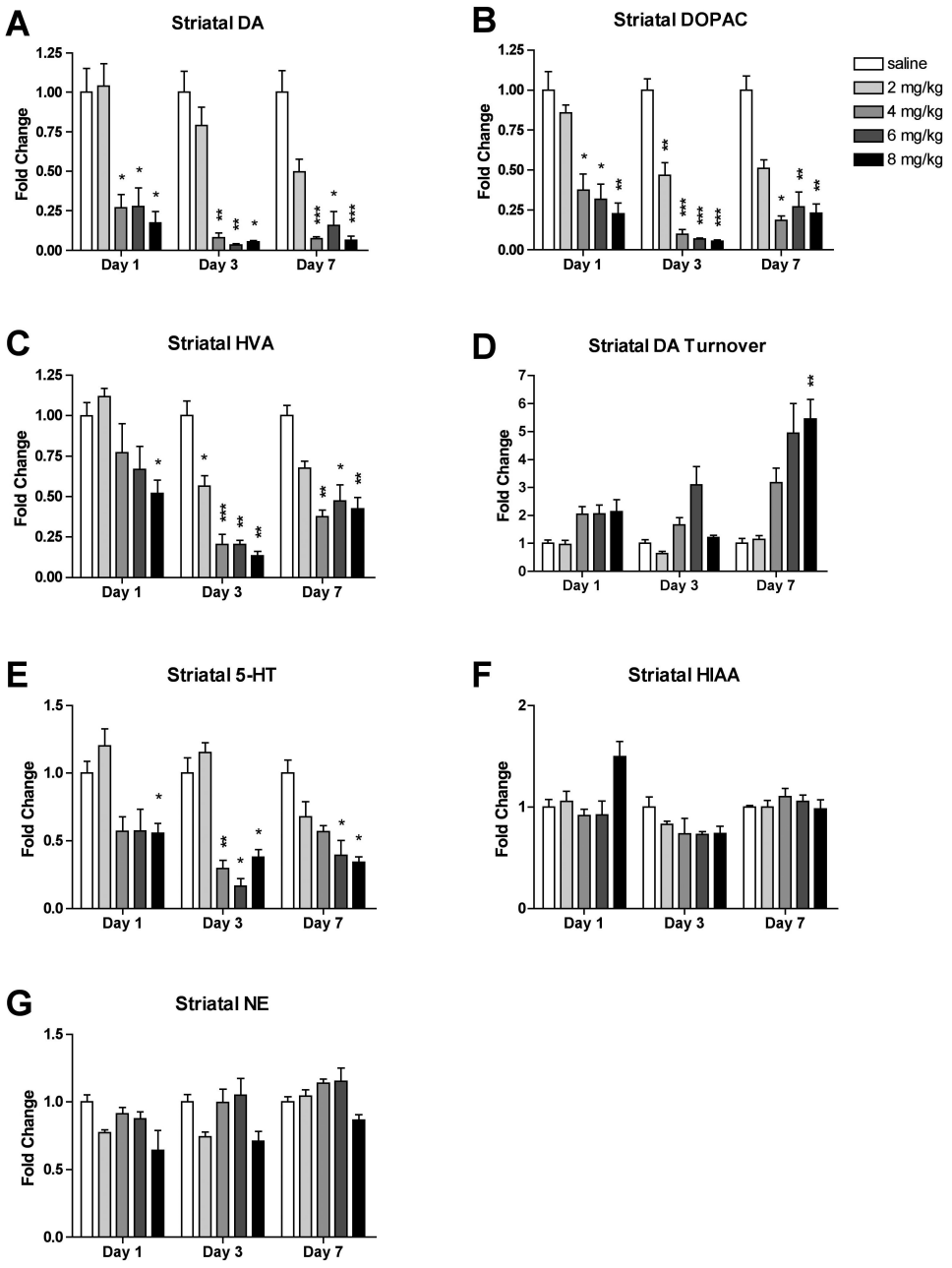

Figure 3.

Binge MA dosing alters levels of striatal monoamines and their metabolites. MA dose-dependently induced rapid and persistent decreases in striatal DA (A), DOPAC (B), and HVA levels (C), and increased DA turnover rates (D) at day 7. Binge MA also diminished striatal 5-HT (E). Striatal HIAA (F) and NE (G) were not significantly affected by binge MA. Data are presented as mean fold change from respective saline + SEM (n = 4-8 per dose group per day). * $p < 0.05$, ** $p < 0.01$, *** $p < 0.001$ compared with saline of the same time point.

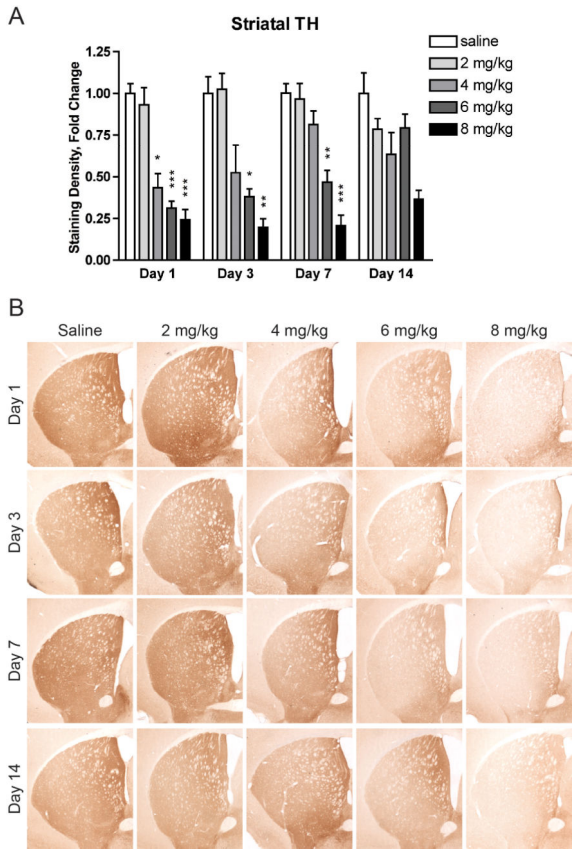

Figure 4.

Binge MA dosing dose-dependently decreases striatal TH levels. (A) Mice given at least 4 mg/kg MA had significantly decreased striatal TH one day after MA treatment. Mice given 6 or 8 mg/kg MA had significantly decreased striatal TH levels for 7 days after MA treatment. Data are presented as mean fold change from respective saline + SEM (n = 5-8 per dose group per day). * $p < 0.05$, ** $p < 0.01$, *** $p < 0.001$ compared with saline group of the same time point. (B) Representative images of tissue immunostained for TH taken at Bregma 0.3 ± 0.2 mm.

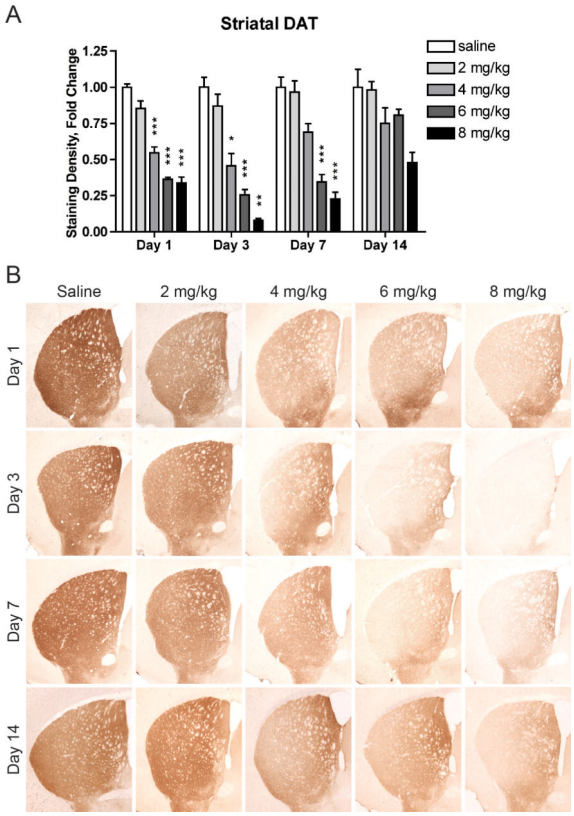

Figure 5.

Binge MA dosing dose-dependently decreases striatal DAT levels. (A) Mice given at least 4 mg/kg MA had significantly decreased striatal DAT levels for at least 3 days. Striatal DAT levels in mice given 6 or 8 mg/kg MA remained significantly diminished for at least 7 days. Data are presented as mean fold change from respective saline + SEM (n = 5-8 per dose group per day). * $p < 0.05$, ** $p < 0.01$, *** $p < 0.001$ compared with saline group of the same time point. (B) Representative images of tissue immunostained for DAT taken at Bregma 0.3 ± 0.2 mm.

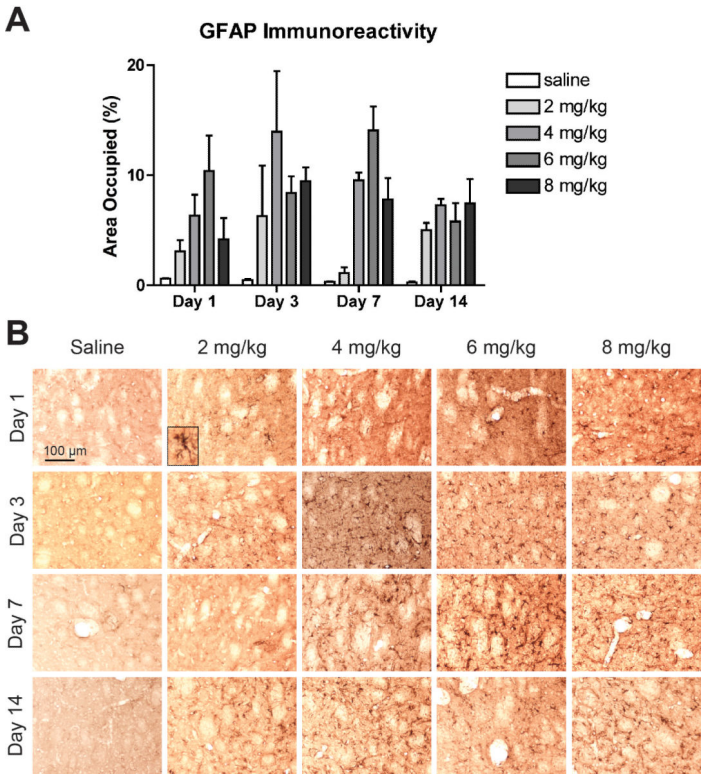

Figure 6.

Binge MA dosing activates striatal astrocytes. (A) MA treatment increased the area occupied by GFAP immunoreactivity compared to saline beginning as early as one day after MA treatment and persisting for at least 14 days. Data are presented as mean + SEM (n = 3 per dose group per day). (B) Astrocyte activation is evident from the increased number of GFAP-positive astrocytes and the cells' activated morphology, exhibiting hypertrophy and increased GFAP immunoreactivity (see inset). Representative images of tissue immunostained for GFAP taken at 20x magnification from the central striatum at Bregma 0.3 ± 0.2mm.

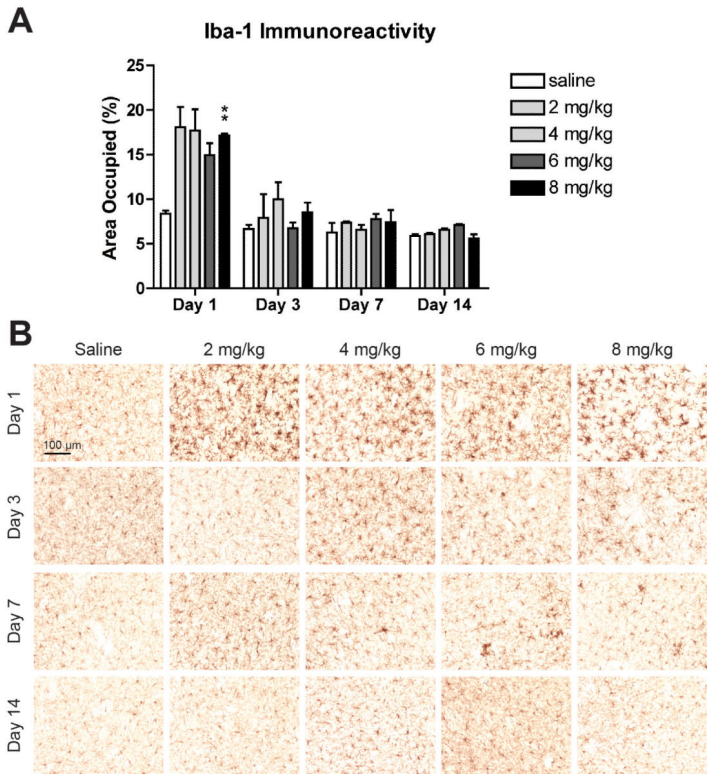

Figure 7.

Binge MA dosing activates striatal microglia. (A) MA treatment increased the area occupied by Iba-1 immunoreactivity compared to saline one day after treatment, though only the highest dose group achieved statistical significance. This increase in area occupied did not persist. Data are presented as mean + SEM (n = 3 per dose group per day). ** $p < 0.01$. (B) All doses of MA induced pronounced microglial activation one day after MA treatment, as evidenced by larger cell bodies, thicker processes, and intense Iba-1 immunoreactivity. This activation diminished over the following days, leaving clusters of activated cells scattered throughout the striatum on day 7. By day 14, the microglial activation had subsided. Representative images of tissue immunostained for Iba-1 taken at 20× magnification from the central striatum at Bregma 0.3 ± 0.2mm.

Table 1

A summary of the changes seen in markers of neurotoxicity and neuroinflammation for each dose and time point.

	Day 1	Day 3	Day 7	Day 14
2 mg/kg	DA: NC	DA: NC	DA: NC	
	TH: NC	TH: NC	TH: NC	TH: NC
	DAT: NC	DAT: NC	DAT: NC	DAT: NC
	GFAP: (↑)	GFAP: (↑)	GFAP: (↑)	GFAP: (↑)
	Iba-1: (↑)	Iba-1: NC	Iba-1: NC	Iba-1: NC
4 mg/kg	DA: ↓	DA: ↓	DA: ↓	
	TH: ↓	TH: NC	TH: NC	TH: NC
	DAT: ↓	DAT: ↓	DAT: NC	DAT: NC
	GFAP: (↑)	GFAP: (↑)	GFAP: (↑)	GFAP: (↑)
	Iba-1: (↑)	Iba-1: NC	Iba-1: NC	Iba-1: NC
6 mg/kg	DA: ↓	DA: ↓	DA: ↓	
	TH: ↓	TH: ↓	TH: ↓	TH: NC
	DAT: ↓	DAT: ↓	DAT: ↓	DAT: NC
	GFAP: (↑)	GFAP: (↑)	GFAP: (↑)	GFAP: (↑)
	Iba-1: NC	Iba-1: NC	Iba-1: NC	Iba-1: NC
8 mg/kg	DA: ↓	DA: ↓	DA: ↓	
	TH: ↓	TH: ↓	TH: ↓	TH: (↓)
	DAT: ↓	DAT: ↓	DAT: ↓	DAT: (↓)
	GFAP: (↑)	GFAP: (↑)	GFAP: (↑)	GFAP: (↑)
	Iba-1: ↑	Iba-1: NC	Iba-1: NC	Iba-1: NC

Up and down arrows indicate statistically significant changes, compared with the saline-treated group of the same time point. Arrows in parentheses indicate changes of two-fold or greater for which a significant main effect of MA was revealed by twoway ANOVA, but that did not reach statistical significance in pairwise comparisons with the saline-treated group of the same time point. NC indicates no change.